

Photonic crystal waveguides with semi-slow light and tailored dispersion properties

Lars H. Frandsen, Andrei V. Lavrinenko, Jacob Fage-Pedersen, and Peter I. Borel

COM•DTU, Department of Communications, Optics & Materials, Nano•DTU,
Technical University of Denmark, DK-2800 Kgs Lyngby, Denmark
lhf@com.dtu.dk, ala@com.dtu.dk, fage@com.dtu.dk, pib@com.dtu.dk

Abstract: We demonstrate a concept for tailoring the group velocity and dispersion properties for light propagating in a planar photonic crystal waveguide. By perturbing the holes adjacent to the waveguide core it is possible to increase the useful bandwidth below the light-line and obtain a photonic crystal waveguide with either vanishing, positive, or negative group velocity dispersion and semi-slow light. We realize experimentally a silicon-on-insulator photonic crystal waveguide having nearly constant group velocity $\sim c_0/34$ in an 11-nm bandwidth below the silica-line.

©2006 Optical Society of America

OCIS codes: (230.7390) Waveguides, planar; (260.2030) Dispersion, (999.9999) Photonic crystals, (999.9999) Group Velocity.

References and links

1. S. G. Johnson, P. R. Villeneuve, S. Fan, and J. D. Joannopoulos, "Linear waveguides in photonic crystal slabs," *Phys. Rev. B* **62**, 8212-8222 (2000).
2. M. Soljacic, S. G. Johnson, S. Fan, M. Ibanescu, E. Ippen, and J. D. Joannopoulos, "Photonic-crystal slow-light enhancement of nonlinear phase sensitivity," *J. Opt. Soc. Am. B* **19**, 2052-2059 (2002).
3. R. S. Jacobsen, K. Andersen, P. I. Borel, J. Fage-Pedersen, L. H. Frandsen, O. Hansen, M. Kristensen, A. Lavrinenko, G. Moulin, H. Ou, C. Peucheret, B. Zsigri and A. Bjarklev, "Strained silicon as a new electro-optic material," *Nature* **441**, 199-202 (2006).
4. M. Notomi, K. Yamada, A. Shinya, J. Takahashi, C. Takahashi, and I. Yokohama, "Extremely large group velocity dispersion of line-defect waveguides in photonic crystal slabs," *Phys. Rev. Lett.* **87**, 253902 (2001).
5. H. Gersen, T. J. Karle, R. J. P. Engelen, W. Bogaerts, J. P. Korterik, N. F. van Hulst, T. F. Krauss, and L. Kuipers, "Real space observations of ultraslow light in photonic crystal waveguides," *Phys. Rev. Lett.* **94**, 073903 (2005).
6. G. Lenz, B. J. Eggleton, C. K. Madsen, and R. E. Slusher, "Optical delay lines based on Optical Filters," *IEEE J. Quantum Electron.* **37**, 525-532 (2001).
7. Y. A. Vlasov and S. J. McNab, "Coupling into the slow light mode in slab-type photonic crystal waveguides," *Opt. Lett.* **31**, 50-52 (2006).
8. J. García, P. Sanchis, and J. Martí, "Detailed analysis of the influence of structure length on pulse propagation through finite-size photonic crystal waveguides," *Opt. Express* **14**, 6879-6893 (2006).
9. S. Hughes, L. Ramunno, J. F. Young, and J. E. Sipe, "Extrinsic optical scattering loss in Photonic Crystal Waveguides: Role of fabrication disorder and photon group velocity," *Phys. Rev. Lett.* **94**, 033903 (2005).
10. R. J. P. Engelen, Y. Sugimoto, Y. Watanabe, J. P. Korterik, N. Ikeda, N. F. van Hulst, K. Asakawa, and L. Kuipers, "The effect of higher-order dispersion on slow light propagation in photonic crystal waveguides," *Opt. Express* **14**, 1658-1672 (2006).
11. K. Yamada, H. Morita, A. Shinya, and M. Notomi, "Improved line-defect structures for photonic-crystal waveguides with high velocity," *Opt. Commun.* **198**, 395-402 (2001).
12. A. Jafarpour, A. Adibi, Y. Xu, and R. K. Lee, "Mode dispersion in biperiodic photonic crystal waveguides," *Phys. Rev. B* **68**, 233102 (2003).
13. A.Y. Petrov, and M. Eich, "Zero dispersion at small group velocities in photonic crystal waveguides," *Appl. Phys. Lett.* **85**, 4866-4868 (2004).
14. G. P. Agrawal, *Fiber-Optic Communication Systems* (Wiley-Interscience, 1997).
15. S. Johnson and J. Joannopoulos, "Block-iterative frequency-domain methods for Maxwell's equations in a planewave basis," *Opt. Express* **8**, 173-190 (2001).
16. R. Jacobsen, A. Lavrinenko, L. Frandsen, C. Peucheret, B. Zsigri, G. Moulin, J. Fage-Pedersen, and P. Borel, "Direct experimental and numerical determination of extremely high group indices in photonic crystal waveguides," *Opt. Express* **13**, 7861-7871 (2005).
17. M. Settle, M. Salib, A. Michaeli, and T. F. Krauss, "Low loss silicon on insulator photonic crystal waveguides made by 193nm optical lithography," *Opt. Express* **14**, 2440-2445 (2006).

1. Introduction

The intricate confinement of light in a photonic crystal waveguide (PhCW) [1] and its resulting dispersion properties offer sophisticated possibilities for realizing complex nanophotonic circuits. Potentially, PhCWs may facilitate delay lines for package synchronization, dispersion compensation, and enhanced light-matter interactions [2, 3] in nanophotonic circuits by exploiting slow-light phenomena [4]. However, the practical utilization of *ultra*-slow light reaching group velocities below $\sim c_0/200$ [3,5] in PhCWs may be limited due to an inherent small bandwidth [6], impedance mismatch [7, 8], intensified loss mechanisms at scattering centers [9], and extreme dispersive pulse broadening [4, 10]. Previously, it has been demonstrated that the dispersion properties of PhCWs can be altered via a structural tuning of the waveguide geometry, typically, by changing the waveguide width or by introducing bi-periodicity [11, 12, 13]. However, such dramatic changes of the PhCW may lead to multimode operation, decreased coupling efficiency to a photonic wire, and structural continuity problems in, e.g., bend and splitting regions. Here, we show how the knowledge of the field distributions in a single-line defect (W1) PhCW can be exploited to tailor the dispersion properties of the fundamental even photonic bandgap (PBG) mode. In this way, one can realize a silicon-on-insulator (SOI) W1 PhCW with semi-slow light having a group velocity in the range $\sim(c_0/15 - c_0/100)$; vanishing, positive, or negative group velocity dispersion (GVD); and low-loss propagation in a practical ~ 5 -15 nm bandwidth.

2. Design aspects & modeling

The group velocity v_g of light with frequency ω in an optical waveguide is given as [14]:

$$v_g = \frac{d\omega}{dk} = \frac{c_0}{n_g}, \quad (1)$$

where k is the wavevector along the waveguide and n_g the group index. The dispersion relations $\omega(k)$ for a given waveguide system can easily be obtained numerically by using e.g. the plane wave expansion (PWE) method. Hereafter, it is straightforward to obtain v_g by numerical differentiation according to Eq. (1). The group velocity in a PhCW is strongly dependent on the frequency [6] as quantified by the GVD parameter β_2 , given by the second order derivative of the dispersion relation [14]:

$$\beta_2 = \frac{d^2k}{d\omega^2} = \frac{dn_g}{d\omega} \frac{1}{c_0}. \quad (2)$$

Figure 1(a) shows a typical band diagram for transverse-electric (TE) polarized light in a 2D W1 PhCW which is realized in silicon by arranging air holes of diameter $D = 0.6\Lambda$ in a triangular lattice with pitch Λ . The normalized dispersion relations are found for wavevectors k_z along the direction of the waveguide core [15], which is formed by introducing a single line-defect in the nearest-neighbor direction of the lattice. The inset of Fig. 1(a) shows the supercell used in the PWE calculation. As seen, the W1 PhCW supports one even (solid black) and one odd (dashed black) mode in the PBG which is located at frequencies $\sim (0.20 - 0.28) \Lambda/\lambda$. The parities of the modes are defined by their in-plane symmetry with respect to the waveguide core. The even PBG mode is seen to flatten for $k_z \geq 0.3$ and, eventually, obtains a zero slope at $k_z = 0.5$. This is due to the folding at the Brillouin zone-end [1]. Figure 1(b) shows the resulting group velocity v_g for the even PBG mode (black) calculated by using Eq. (1). It reveals a dramatic reduction in v_g for increasing wavevectors (lower frequencies). As expected, the group velocity $v_g \approx c_0/4$ is close to that of light propagating in a conventional silicon waveguide (with $n_{\text{Si}} \approx 3.5$) for $k_z \lesssim 0.3$. For $k_z \geq 0.3$, v_g decreases monotonically below $c_0/20$. Near $k_z = 0.5$, v_g approaches zero, hence, addressed as the slow-light regime. Therefore, different frequencies will travel at very different speeds in a W1 PhCW. Correspondingly, the GVD parameter β_2 (red) plotted in Fig. 1(b) increases by several orders of magnitudes from

-10^4 ps²/km to an extreme negative GVD below -10^9 ps²/km in the slow-light regime. Such extreme GVD will distort any pulse-train propagating through the W1 PhCW. Hence, the monotonically changing group velocity along with the extreme GVD in the W1 PhCW will be devastating for the utilization of slow-light in e.g. a wavelength-division multiplexed system.

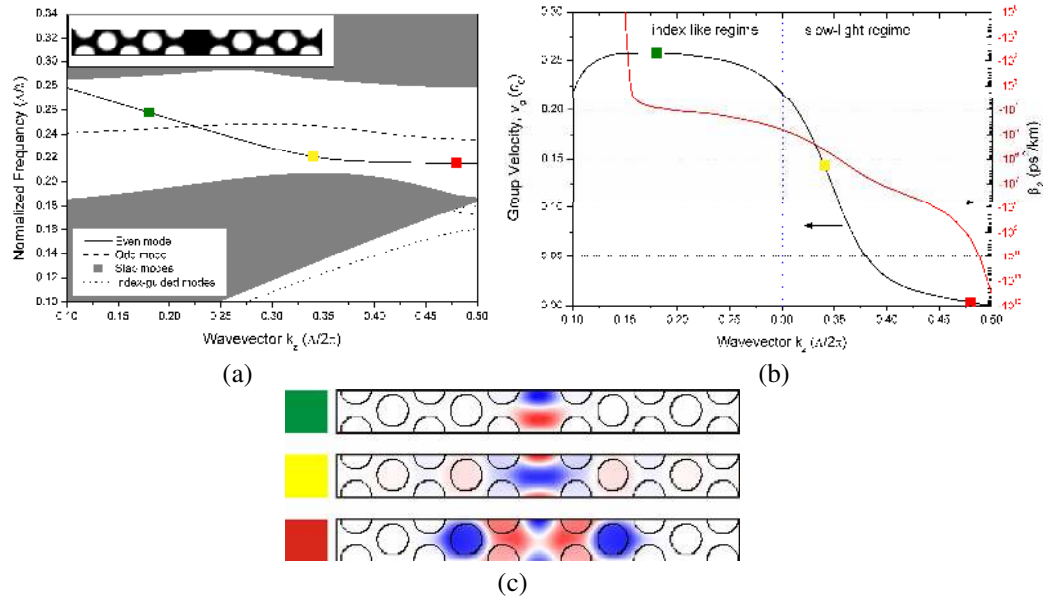


Fig. 1. (a) Typical band diagram showing the normalized frequencies versus normalized wavevectors for a single-line defect 2D photonic crystal waveguide supporting an even (solid) and odd (dashed) mode in the bandgap. The inset of the graph sketches the supercell used in the plane wave expansion calculation. (b) Group velocity v_g in units of the speed of light in vacuum, c_0 , versus wavevector k_z (black), calculated by using Eq. (1). The group velocity dispersion parameter β_2 obtained from Eq. (2) (red). (c) Modal field distributions in a W1 PhCW for the wavevectors marked by a red, yellow, and green square in (a) and (b).

The knowledge of the modal field distribution can be exploited to tailor the dispersion characteristics of the W1 PhCW. Figure 1(c) shows the modal field distributions for the even PBG mode for three different wavevectors marked by the green, yellow, and red squares in Figs. 1(a) and 1(b). For $k_z \lesssim 0.3$ with $v_g \approx c_0/4$ (green square), the mode is seen to be well-confined in the waveguide core and the mode profile looks similar to that of a fundamental mode in a ridge waveguide. Hence, in this index-like regime the mode is usually referred to as being index-guided. Entering the slow-light regime (yellow square), the mode starts to penetrate into the photonic crystal cladding and, eventually, has its field highly concentrated in the first and second row of holes (red square). Thus, the properties of the even PBG mode in the index-like regime depend mainly on the parameters of the first row of holes, whereas the slow-light part of the mode is strongly dependent on the parameters of the photonic crystal cladding, especially, the first two rows of holes. A consequence of this is illustrated in Fig. 2, where the even PBG mode is plotted for a W1 PhCW with bulk hole diameter $D = 0.60\lambda$ and various diameters (a) D_1 of the first row of holes, and (b) D_2 of the second row of holes. Clearly, the mode moves down in frequency in *both* the index-like and slow-light regimes when the diameter D_1 is decreased, as the effective index is increased locally. Moreover, the slope at large wavevectors increases in magnitude and the bandwidth, in which the dispersion relation is linear, increases in the slow-light regime. On the contrary, the mode is only affected at large wavevectors when the diameter D_2 is changed, as only the part of the mode in the slow-light regime ‘feels’ the second row of holes. By decreasing D_2 the slope of the tail increases in magnitude. Thus, the field distributions in Fig. 1(c) nicely document a frequency

dependent behavior of the even PBG mode on the waveguide geometry and can be used as guidelines to selectively tailor the dispersion properties of a W1 PhCW in the slow-light regime.

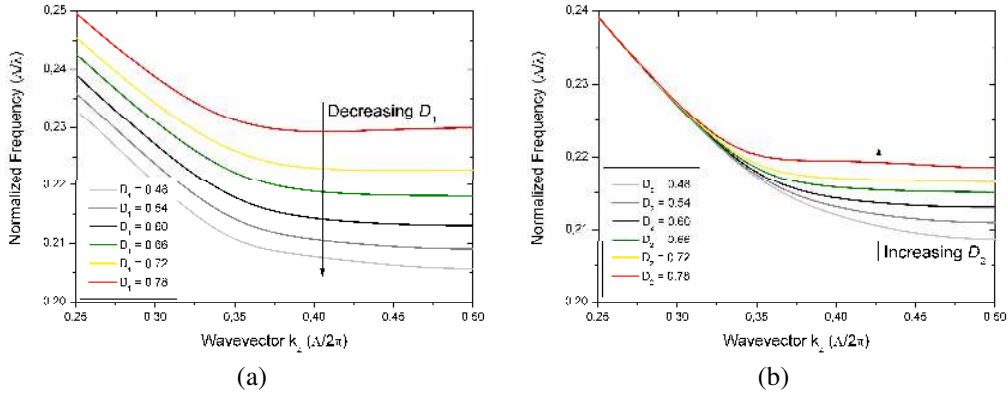


Fig. 2. Movement of the even PBG mode when changing the diameter (a) D_1 of the first row and (b) D_2 of the second row of holes in a W1 PhCW. Bulk holes have diameter $D = 0.60A$.

One design goal for a practical utilization of slow-light in a W1 PhCW could be to obtain *semi-slow* light with a group velocity in the range $\sim(c_0/15 - c_0/100)$ and a vanishing GVD (i.e., a linear dispersion relation) in a $\sim 5\text{-}15$ nm bandwidth. This can be achieved by combining the effects illustrated in Figs. 2(a) and 2(b). By decreasing D_1 , we perform a coarse tuning of v_g , raising it to the desired range and increasing the bandwidth with linear dispersion for large wavevectors k_z . By changing D_2 , we can fine-tune v_g for the tail of the mode, whereby we arrive at the desired group velocity and/or dispersion. Figure 3(a) shows a 3D calculation of the band diagram of the even PBG mode for three examples of perturbed W1 PhCWs. The diameter D_1 has been *decreased* by 30 nm (red), 40 nm (yellow), and 60 nm (green), whereas the diameter D_2 has been *increased* by 60 nm (red), 30 nm (yellow), and 10 nm (green) to obtain different group velocities and GVDs in different bandwidths.

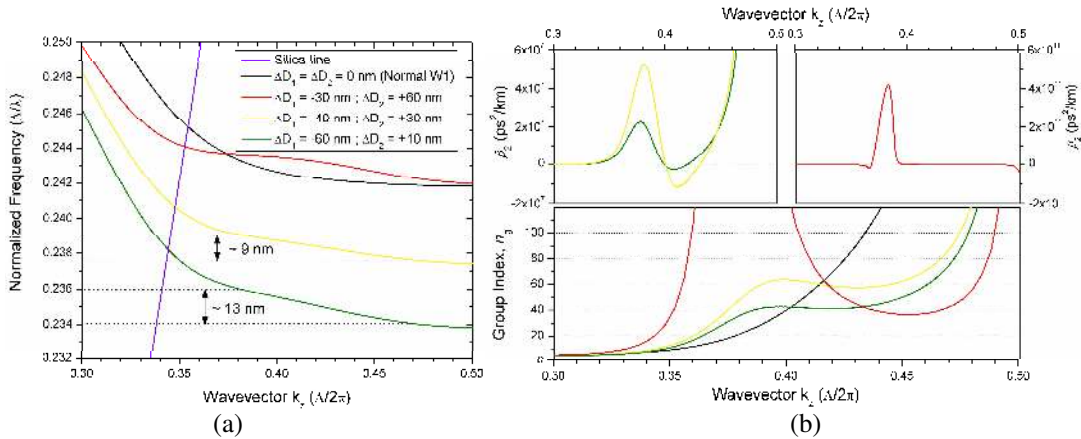


Fig. 3. (a). Band diagram for different even PBG modes in a 3D W1 PhCW where the diameter D_1/D_2 of the first/second row of holes have been changed according to the legend, relative to the bulk diameter $D = 222$ nm. (b) Corresponding calculated group indices (bottom) and group velocity dispersion parameter β_2 (top, left and right) for the modes plotted in (a).

In the PWE calculation, the pitch $\Lambda = 370$ nm and the diameter of the bulk holes $D = 0.60\Lambda = 222$ nm. The structure is set to penetrate a 340-nm layer of silicon placed on a buffer layer of silica and having air above. For comparison, the even mode for the generic W1 PhCW is also plotted (black). As seen, the perturbations represented by the yellow and green curves result in regions with nearly linear dispersion relations situated below the silica-line (violet) and are, thus, vertically confined to the silicon slab. Figure 3(b, bottom) shows the corresponding group indices, n_g [see Eq. (1)], calculated by numerical differentiation of the bands in Fig. 3(a). As seen, the two perturbed PhCWs have plateaus where the group indices are constant within 5% around ~ 40 (green) and ~ 60 (yellow) over bandwidths of roughly ~ 13 nm and ~ 9 nm, respectively. These group-index plateaus are in sharp contrast to the group-index behavior for the generic W1 PhCW (black) that rises monotonically to extreme values. Inspecting the calculated GVD β_2 values in Fig. 3(b, top), we see that the group-index plateaus lead to relatively low and positive GVDs on the order of 10^5 - 10^6 ps²/km (yellow and green curves), which is not much larger in magnitude than in the index-like regime. A finer tuning of the geometry may lead to vanishing GVDs. Furthermore, we see that a perturbation of the W1 PhCW geometry also allows us to realize a PhCW having an extreme *positive* GVD (red curve), i.e. having a negative dispersion [14].

3. Fabrication and experimental results

Figure 4 shows a typical scanning electron micrograph of a fabricated 10- μm long perturbed W1 PhCW, where the diameter D_1/D_2 has been decreased/increased relative to the bulk holes with diameter $D = 234$ nm. The triangular photonic crystal lattice with pitch $\Lambda = 370$ nm penetrates the top 338-nm silicon slab of an SOI wafer having a 1- μm thick buffer layer of silica. The photonic crystal patterns were defined by using electron-beam lithography and transferred to the silicon by inductively coupled plasma reactive ions etching.

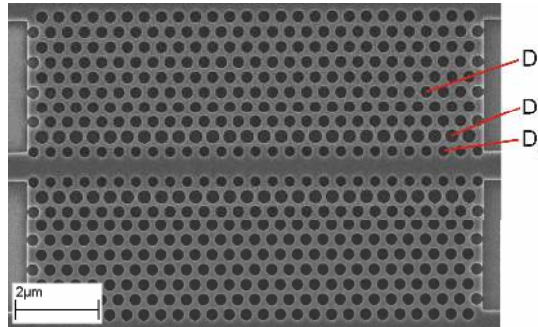


Fig. 4. Scanning electron micrograph of a perturbed photonic crystal waveguide. The diameter D_1/D_2 has been decreased/increased compared to the diameter D of the bulk holes.

Figure 5(a, right) shows the transmission spectrum (gray) measured for TE-polarized light in a 500- μm long perturbed PhCW where the diameters D_1/D_2 have been decreased/increased by ~ 54 nm/ ~ 9 nm. The band diagram for the fabricated structure is plotted in Fig. 5(a, left) with a $\sim 1\%$ blue-shift (solid black). The two transmission peaks of the measured spectrum can easily be correlated to the two linear dispersion regions for the even PBG mode located above (dotted red) and below (dotted green) the silica-line. The group index n_g for light propagating through the 500- μm long perturbed PhCW has been measured experimentally and calculated numerically by using the time-of-flight methods as described in Ref. [16]. Figure 5(b) plots the group index obtained from measurement (black), 2D Finite-Difference Time-Domain calculation (FDTD, blue), and 3D PWE-calculation (red). The 2D FDTD group-index spectrum has been blue-shifted $\sim 12.5\%$ to match the experimental wavelength scale. The group index for the ~ 11 -nm broad transmission peak corresponding to the linear part of the even PBG mode below the silica-line (indicated by the dotted green lines in Fig. 5) has been measured to $n_g = 34 \pm 3$, which is in close agreement with the values predicted by FDTD and

PWE. The obtained uncertainty below 10% of the measured group-index is better compared to the uncertainty obtained in Ref. [16]. This is due to a lower loss and an increased optical path length, i.e. a longer absolute time-of-flight, for the PhCW in the present investigation. The fringes in the FDTD-calculated spectrum are caused by the finite length [8] of the 20- μm long PhCW used in the simulation. The PWE group-index plateau in Fig. 5(b) reveals a positive GVD parameter β_2 on the order of 10^5 - 10^6 ps^2/km , which is of opposite sign and several orders of magnitudes lower than β_2 in the slow-light regime of a W1 PhCW [see Fig. 1(b)]. The propagation loss for the perturbed PhCW has been measured with a typical error of 2-3 dB/mm using the cut-back method with four PhCWs of lengths 50, 100, 500, and 1000 μm and is shown in Fig. 5(b) (green curve). As seen, the propagation loss in the ~ 11 -nm wavelength range is less than ~ 20 dB/mm and drops below 5 dB/mm in a ~ 2 -nm bandwidth from $\sim(0.2385$ - $0.2388)$ Λ/λ . We have fabricated a different set of perturbed PhCWs having a ~ 7 -nm group-index plateau with $n_g = 17 \pm 2$ and showing a propagation loss of 4.2 ± 1.2 dB/mm. The advantage of the perturbed PhCWs is that the losses induced by the silica-line and extreme dispersion are diminished in comparison with W1 PhCWs [17]. Thus, perturbed PhCWs are very promising for the SOI configuration as they offer bandwidth, slow-light, and low losses.

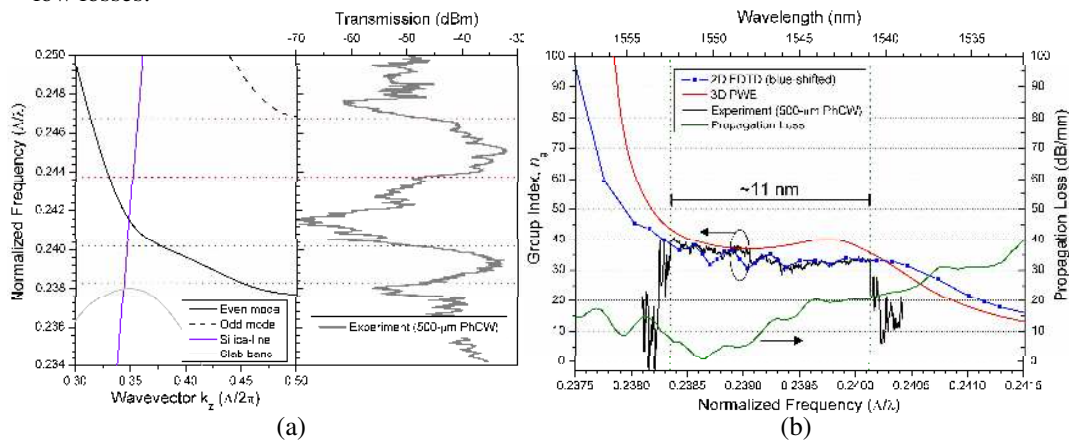


Fig. 5. (a) 3D band diagram (left) and transmission spectrum (right) for a perturbed 500- μm PhCW with $\Delta D_1 = -60$ nm and $\Delta D_2 = +10$ nm. The even PBG mode (solid black) gives rise to two transmission peaks: one located above (dotted red) and one located below (dotted green) the silica-line (violet). (b) Measured (black), 2D FDTD (blue) and 3D PWE (red) calculated group index for the perturbed PhCW. The measured propagation loss is also plotted (green).

4. Conclusion

The field distributions in a single-line defect photonic crystal waveguide have shown to be useful guidelines for tailoring the dispersion relation of the fundamental, even photonic bandgap mode. The tailoring is obtained by doing a simple perturbation to the diameters of the first and second row of holes adjacent to the waveguide core. This general concept can be applied to photonic crystal waveguides of any design. In this way, it is possible to realize waveguides having low-loss bandwidths with semi-low group velocity, and vanishing, negative, or positive group velocity dispersion. We have realized a W1 photonic crystal waveguide in silicon-on-insulator material having an ~ 11 -nm bandwidth below the silica-line with a nearly constant group velocity $\sim c_0/34$ and relatively low and positive group velocity dispersion with β_2 on the order of 10^5 - 10^6 ps^2/km . Within this bandwidth, the measured propagation loss is less than 20 dB/mm and drops below 5 dB/mm in a ~ 2 -nm bandwidth.

With tailored group velocity and dispersion, photonic crystal waveguides become much more attractive for practical applications. The perturbed waveguides offer novel possibilities for realizing compact integrated components used for e.g. pulse shaping, dispersion

compensation, and enhanced non-linear effects. They may also help to understand how propagation losses in photonic crystal waveguides scale with group velocity and dispersion.

Acknowledgment

This work was supported in parts by the Danish Technical Research Council via the PIPE (Planar Integrated PBG Elements) project and by the New Energy and Industrial Technology Development Organization (NEDO) via the Japanese Industrial Technology Research Area.